Research Article

APPLICATION OF CSA ALGORITHM FOR THE PMSM SPEED ESTIMATOR OF THE FOC CONTROL METHOD USING EXTENDED KALMAN FILTER

Thinh Cong TRAN[1,*], *Pavel BRANDSTETTER*[2], *Huynh Tan DE*[3], *Hau Huu VO*[1]

[1]Modeling Evolutionary Algorithms Simulation and Artificial Intelligence, Faculty of Electrical and Electronics Engineering, Ton Duc Thang University, Ho Chi Minh City, Vietnam
[2]Faculty of Electrical Engineering and Computer Science, VSB–Technical University of Ostrava, Ostrava City, Czech Republic
[3]Faculty of Electrical and Electronics Engineering, Ton Duc Thang University, Ho Chi Minh City, Vietnam

trancongthinh@tdtu.edu.vn, pavel.brandstetter@vsb.cz, huynhtande@tdtu.edu.vn, vohuuhau@tdtu.edu.vn

*Corresponding author: Thinh Cong Tran; trancongthinh@tdtu.edu.vn

DOI: 10.15598/aeee.vxxix.241108

Article history: Received Nov 13, 2024; Revised Apr 15, 2025; Accepted Apr 20, 2025; First Published May 20, 2025.

Abstract. *Nowadays, Permanent Magnet Synchronous Motors (PMSM) are used more and more widely due to their advantages over other types of motors, such as high efficiency, constant torque, higher power density, and wide speed range. Many studies on this motor have been carried out in the industry. This paper proposes an application for the PMSM motor to estimate the speed of the motor rotor using an extended Kalman filter (EKF). This also means that the motor is controlled without using a speed sensor, so the system has the advantages of reducing the cost of manufacturing encoders, less damage, increased reliability, and reduced size due to the absence of moving mechanical parts of the sensor. The estimated performance depends heavily on the parameters of the covariance matrices in the filter. In the paper, the filter parameters are optimized using the Cuckoo Search Algorithm (CSA). The simulation results of the proposed algorithm on the PMSM motor show its advantages over traditional methods.*

Keywords

EKF, FOC control, CSA algorithm, PMSM, Speed estimation, Sensorless, MRAS, noise.

1. Introduction

Currently, Permanent Magnet Synchronous Motors (PMSM) have many advantages compared to other types of motors, so many studies on the PMSM motor have been carried out, such as speed control according to V/F frequency, torque control (DTC) and vector control (FOC). There is also interest in sensorless speed control. Sensorless control has the following advantages: saving components, increasing durability, and stabilizing motor operation.

There have been some studies on speed estimation, such as model reference adaptive system (MRAS) [1–5]. The MRAS model compares the outputs of two models: the first part (reference mode does not include the rotor speed; the second part (adaptive model) uses the speed to estimate the induction motor flux. The output values of these two parts are compared to each other to get the error. The error is injected into the adaptation mechanism to produce a rate estimate that feeds back into the adaptation typical. This model's features include simplicity and speed of processing, but it also has significant errors.

The sliding mode standard has been used to estimate and monitor when there are uncertainties. The sliding observer (SMO) [6–9] was effective in estimating unknown inputs or errors. Several first-order sliding mode observers have been applied in the industry for speed sensorless estimation and control. Many speed estimation models require low-pass filtering and extra position compensation for the PMSM motor's rotor.

The speed estimation method uses intelligent algorithms such as neural networks [10–12]. Neural networks are one branch of smart control technology. A radial basis function (RBF) neural network is a network that has a three-layer sequential architecture. It can establish a good nonlinear mechanism. For each training sample, it only needs to change a small weight value. Its advantages are fast convergence speed and small errors. Some studies estimate speed using EKF filters with Q and R matrices selected by the True-False method will take a lot of time and the accuracy in speed estimation is not high [13–16]. Some papers propose ways to determine the parameters of the covariance matrix using the GA and the PSO algorithms [19] and [21]. In those algorithms, the CSA algorithm proves more effective in finding the optimal parameters with the same number of iterations and population sizes [19]. This article proposes a sensorless method for the FOC model of a PMSM motor using an EKF filter in which the Q and R matrices are optimized using the Kucoo Search Algorithm. This article also compares the response when the Q and R matrices are arbitrarily chosen, selected using the True-False method, and the case is optimized using the CSA algorithm.

2. The FOC Model of the PMSM Motor

Tab. 1: The Nomenclatures of the State Space Equations

I_d, I_q	The current components of the real and imaginary parts of the current vector in the rotor reference frame (d-q)
V_d, V_q	The voltage components on the reference frame (d-q)
R_s	The stator resistance
L_d, L_q	The stator inductances at the pole along and across the pole (d-q)
T_e	The motor torque
T_L	The load torque
Ω	The rotor angular velocity
θ	The rotor rotation angle
P	Number of pole pairs
J	Moment of inertia
C_f	The friction coefficient

The PMSM continuous model in the d-q reference frame can be expressed as follows:

$$\begin{cases} L_d\frac{dI_d}{dt} = V_d - R_sI_d + P\Omega L_qI_q \\ L_q\frac{dI_q}{dt} = V_q - R_sI_q - P\Omega(L_dI_d + \psi) \\ J\frac{d\Omega}{dt} = T_e - T_L - C_f\Omega \\ \frac{d\theta}{dt} = \Omega \end{cases} \tag{1}$$

The expression can be rewritten in matrix form below.

$$\frac{d}{dt}\begin{bmatrix} I_d \\ I_q \\ \Omega \\ \theta \end{bmatrix} = \begin{bmatrix} \frac{-R_s}{L_d} & \frac{P\Omega I_q}{L_d} & 0 & 0 \\ \frac{-P\Omega I_d}{L_q} & \frac{-R_s}{L_q} & \frac{-P\psi}{L_q} & 0 \\ 0 & \frac{3P\psi}{2J} & \frac{-C_f}{J} & 0 \\ 0 & 0 & 1 & 0 \end{bmatrix}\begin{bmatrix} I_d \\ I_q \\ \Omega \\ \theta \end{bmatrix} + \begin{bmatrix} \frac{1}{L_d} & 0 & 0 \\ 0 & \frac{1}{L_q} & 0 \\ 0 & 0 & \frac{-1}{J} \\ 0 & 0 & 0 \end{bmatrix} 0 \begin{bmatrix} V_d \\ V_q \\ T_L \end{bmatrix} \tag{2}$$

We have the currents I_d, I_q.

$$\begin{bmatrix} I_d \\ I_q \end{bmatrix} = \begin{bmatrix} 1 & 0 & 0 & 0 \\ 0 & 1 & 0 & 0 \end{bmatrix}\begin{bmatrix} I_d & I_q & \Omega & \theta \end{bmatrix}^T \tag{3}$$

The state space equations (2) and (3) are abbreviated as follows:

$$\begin{cases} \dot{x} = A.x + B.u \\ y = C.x \end{cases} \tag{4}$$

With the equation system of the PMSM motor (4), a sensorless field-oriented speed controller for the PMSM motor is built in Fig. 1. The Kucoo research algorithm is proposed in this architecture. The speed estimator uses an extended Kalman filter (CSA-EKF) whose input parameters are current and voltage acquired from the model through current and voltage sensors. The motor's estimated speed and rotation angle are its outputs.

The Field Oriented Control (FOC) consists of two stator current components characterized by a vector. The method is based on converting a three-phase speed and time structure into a two-coordinate (d and q) time-invariant structure. This scheme creates an arrangement similar to the DC motor controller. The vector controller requires two parameters as input references: the torque and current component, the I_d component described by the flux current and the I_q component described by the rotor speed [18].

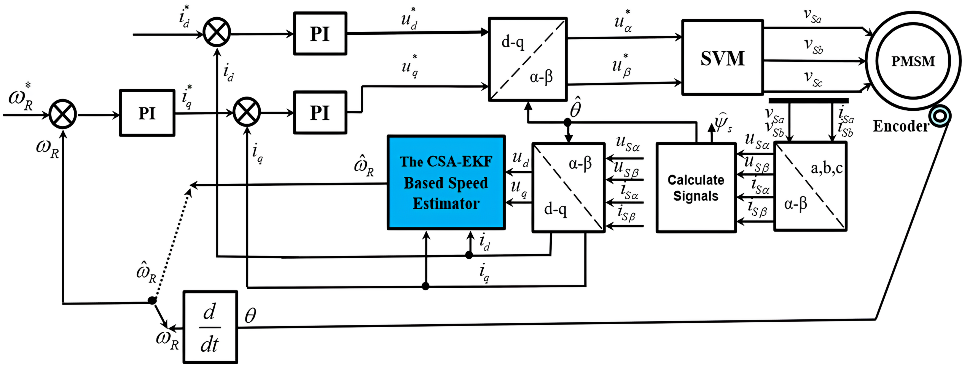

Fig. 1: The organization of the FOC method for PMSM motor.

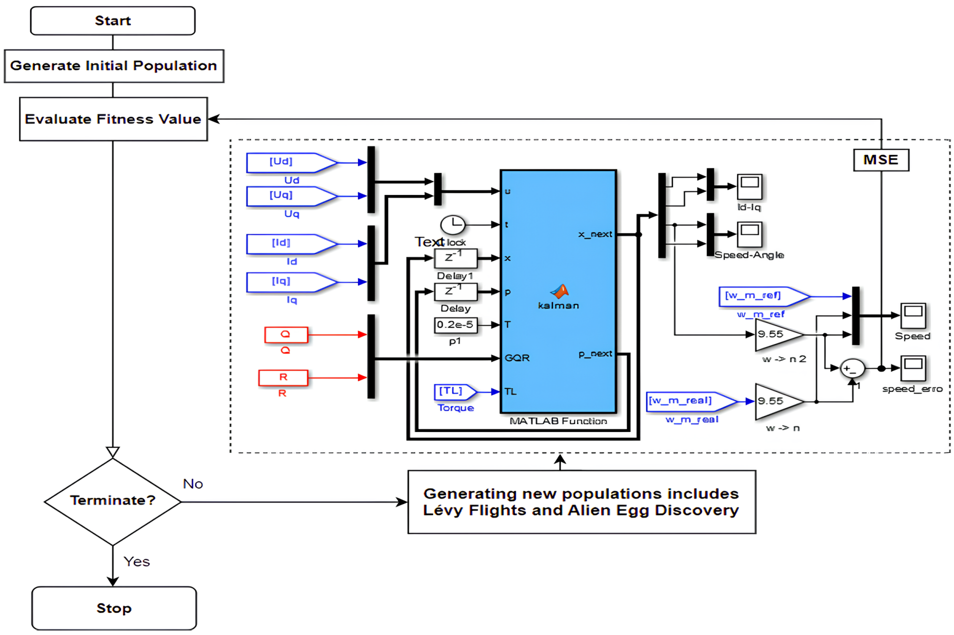

Fig. 2: The flow chart of the Cuckoo Search Algorithm for CSA-EKF method of PMSM.

3. Estimate the Speed of PMSM Using the EKF Optimized through CSA Algorithm

This section begins by presenting the equations of state in their discrete form. The next part is the algorithm of the extended Kalman filter and identifies variables of the matrix Q in the system model, and the matrix R in the measurement block. The disadvantages of determining the matrix Q and R with the trial and error method. Lastly, the CSA algorithm is utilized to fix the optimal values of the variables in the matrix Q, and R for estimating the speed of the PMSM.

3.1. Using the EKF for the speedy estimation of the PMSM

From (4), after adding the disturbance components, we have the extended state model:

$$\dot{x} = A.x + B.u + w(t) \tag{5}$$

$$y = C.x + v(t) \tag{6}$$

The PMSM motor's nonlinear equations (5) and (6) of extended state space will be discretized, making each tiny step regarded as linear, and the Kalman algorithm will be used. To estimate the parameters of the state equation for the PMSM motor, this is a recursive problem with adaptation.

$$\mathbf{x}_{n+1} = \mathbf{A}_n \cdot \mathbf{x}_n + \mathbf{B}_n \cdot \mathbf{u}_n + W_n \tag{7}$$

$$\mathbf{y}_{n+1} = \mathbf{C}_n \cdot \mathbf{x}_{n+1} + V_n \tag{8}$$

With $A_n = e^{AT} \approx I + AT$; $B_n = \int\limits_0^T e^{AT} B dt = BT$; $C_n = C$.

In addition, the components of the equation of state are determined by the following expressions: $x_{n+1} = \begin{bmatrix} i_d^{(n+1)} & i_q^{(n+1)} & \Omega^{(n+1)} & \theta^{(n+1)} \end{bmatrix}^T$;
$y_{n+1} = \begin{bmatrix} i_d^{(n+1)} & i_q^{(n+1)} \end{bmatrix}^T$;
$u_n = \begin{bmatrix} v_d^{(n)} & v_q^{(n)} & T_L \end{bmatrix}^T$;
$A_n = \begin{bmatrix} 1 - \frac{R_s}{L_d}T & p\Omega\frac{L_q}{L_d}T & 0 & 0 \\ -p\Omega\frac{L_q}{L_d}T & 1 - \frac{R_s}{L_q}T & -p\frac{\psi}{L_q} & 0 \\ \frac{3p}{2J}(L_d - L_q)I_qT & \frac{3p}{2J}\psi T & 1 - \frac{C_f}{J}T & 0 \\ 0 & 0 & T & 1 \end{bmatrix}$;
$B_n = \begin{bmatrix} \frac{T}{L_d} & 0 & 0 \\ 0 & \frac{T}{L_q} & 0 \\ 0 & 0 & -\frac{T}{J} \\ 0 & 0 & 0 \end{bmatrix}$; $C_n = \begin{bmatrix} 1 & 0 \\ 0 & 1 \\ 0 & 0 \\ 0 & 0 \end{bmatrix}^T$.

The covariance matrices Q and R of noises obligate the behind formula:
$Q_n = Cov(w) = E[ww^t] = \begin{cases} Q_n with n = l \\ 0 otherwise \end{cases}$;
$R_n = Cov(v) = E[vv^t] = \begin{cases} R_n with n = l \\ 0 otherwise \end{cases}$

The diagonal matrix form is indicated by the matrices Q and R. The PMSM motor speedy estimation model is based on the EKF algorithm [14].

$$\overline{x}_{n+1} = A\widehat{x}_n + Bu_n = f(x_i^n, u^n) \tag{9}$$

The linearization of the nonlinear equation [14] is performed with the following estimated values ($\widehat{x}_i$):

$$F_n = \frac{\partial f_n(x_i^n, u^n)}{\partial x_i} = \frac{\partial(A\widehat{x}_{n-1} + Bu_{n-1})}{\partial x_i} \tag{10}$$

$$\overline{P}_{n+1} = F_n\widehat{P}_nF_n^T + Q \tag{11}$$

$$h(x_i^n) = C_n(x_i^n)x_i^n \tag{12}$$

$$H_n = \frac{\partial h(x_i^n)}{\partial x_i} = \frac{\partial(C_n(x_i^n)x_i^n)}{\partial x_i} \tag{13}$$

$$K_{n+1} = \overline{P_{n+1}}H^T(H\overline{P_{n+1}}H^T + R)^{-1} \tag{14}$$

$$\widehat{x}_{n+1} = \overline{x}_{n+1} + K_{n+1}(y_{n+1} - C_n\overline{x}_{n+1}) \tag{15}$$

$$\widehat{P_{n+1}} = \overline{P_{n+1}} - K_{n+1}C\overline{P_{n+1}} \tag{16}$$

Where the components with a hat represent the estimated values, the noise matrix Q and R are the state variables (parameters) of the PMSM, P is the covariance matrix, and K is the Kalman filter gain. The covariance error matrix's creation values have the formula:

$Q = \begin{bmatrix} \lambda_1 & 0 & 0 & 0 \\ 0 & \lambda_2 & 0 & 0 \\ 0 & 0 & \lambda_3 & 0 \\ 0 & 0 & 0 & \lambda_4 \end{bmatrix}$; $R = \begin{bmatrix} \mu_1 & 0 \\ 0 & \mu_2 \end{bmatrix}$;
$P = \begin{bmatrix} 1 & 0 & 0 & 0 \\ 0 & 1 & 0 & 0 \\ 0 & 0 & 1 & 0 \\ 0 & 0 & 0 & 1 \end{bmatrix}$

An important difficult in the Kalman filter is the parameter determination (λ_i, μ_i) in covariance matrixes Q and R. Normally, these matrices are typically found by trial and error, but this process is laborious and prone to significant errors.

3.2. Using the CSA algorithm to find the optimal parameters of Q, R of the EKF

Due to the limitations of the trial and error method, in this section, the optimal parameters are found using the CSA algorithm [19, 20]. Estimating the speed of the PMSM motor will be more accurate when the parameters are selected appropriately. The algorithm flow chart for finding optimal parameters of matrices Q and R is presented in Fig. 2.

At the beginning of the algorithm, parameters Q and R are initialized randomly and are encoded as real numbers. For simulation, these parameters will be imported into the Matlab model. A cost function will be used to assess its outcomes, followed by experiments like alien egg discovery and the creation of new solutions through Lévy flights. Consequently, we will continue to feed the model for testing with a fresh set of values that are frequently superior to the prior set. Until the necessary number of generations is reached, this process keeps going. The final run time produced the best results.

4. Results and Discussion

The PMSM drive was simulated using MATLAB-SIMULINK. The main parameters of the PMSM are P= 1.5 Kw, P_p= 3, R_S= 0.05 Ω, L_d = 0.0003 H, L_q= 0.0003 H, ψ= 0.027, J= 0.0039 Kg.m^2, C_f = 0.000 N.m.s/rad.

PMSM Driver Parameters: P_N = 1.5 kW, U_{1N}= 220 V, I_{1N} = 4.5 A, n_N = 2500 rev·min^{-1}.

PMSM Parameters: P_N = 1.5 kW, U_{1N}= 220 V, I_{1N} = 3.5 A, n_N = 1500 rpm, P_p= 3, R_S= 0.05 Ω, L_d = 0.0003 H, L_q= 0.0003 H, ψ= 0.027, J= 0.0039 Kg.m^2, C_f = 0.000 N.m.s/rad.

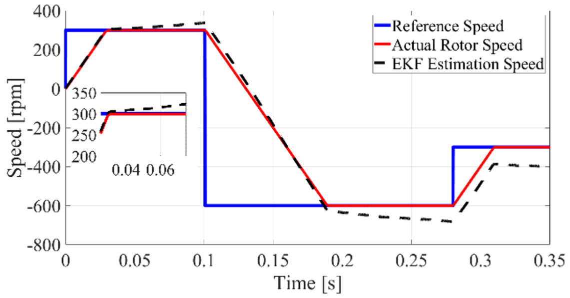

Fig. 3: The comparison of EKF estimation speed with Q_1, R_1 (trial and error) and actual rotor speed.

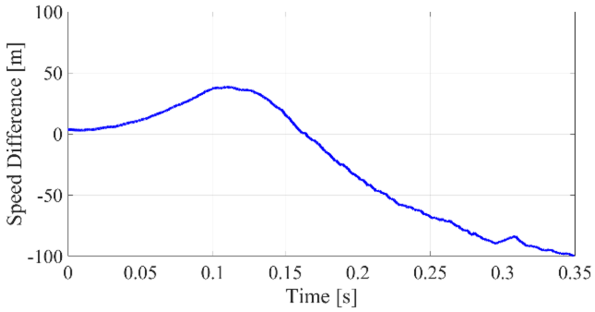

Fig. 4: The error between EKF estimation speed with Q_1, R_1 (trial and error) and actual rotor speed.

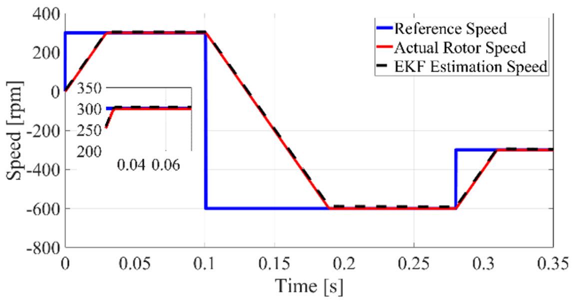

Fig. 5: The comparison of EKF estimation speed with Q_2, R_2 (trial and error) and actual rotor speed.

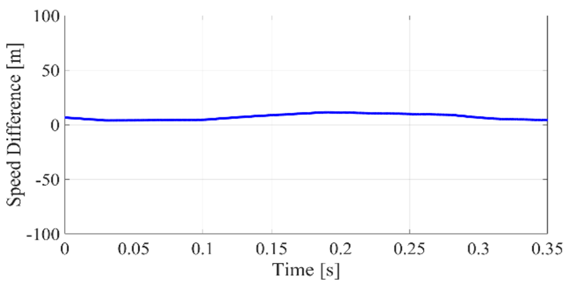

Fig. 6: The error between EKF estimation speed with Q_2, R_2 (trial and error) and actual rotor speed.

4.1. The speed estimation of PMSM based on the EKF filter with Q, R matrix is determined through trial and error

With the trial and error method, we only choose a few times. First, the values Q_1 (10 10 0.01 0.005) and R_1 (100, 1) are chosen, the speed response and speed deviation with these values are shown in Fig. 3 and Fig. 4.

We see that the speed deviation is quite large (the error according to the MSE standard is 2953.04194). In many cases, if the value is not suitable, the speed response will have a larger deviation.

The trial and error method is applied repeatedly to find a better speed response. After more than 15 test times, the parameters Q_2 (10 10 0.0001 0.0001) and R_2 (1, 1) are selected. The speed response with this parameter is shown in Fig. 5 and Fig. 6.

In Fig. 5 and 6, the speed response has improved significantly. In this case, the MSE standard error is 55.75929. The speed response of the PMSM motor is much better than the case in which the Q and R matrices are randomly selected.

4.2. The speed estimation of PMSM based on EKF with Q, R matrix is determined through CSA algorithm

The limitation of trial and error is that it is time-consuming, but the response is not the best. Here, the smart algorithm is applied (CSA algorithm) to find the best set of parameters in a number of iterations. Tab. 2 is the parameters for the CSA algorithm to find optimal parameters for matrices Q and R.

Tab. 2: Parameters of CSA algorithm.

The parameters	The values
Population size	25
The probability of alien egg	0.1
Number of generation	20

The CSA algorithm is performed with 20 iterations. We obtain the results in Tab. 3 and the graph in Fig. 7.

In the first iteration, the algorithm found a pretty good value. The later it gets, the better value it finds. The error is the smallest in the last iteration. The speed error is computed using the MSE error in the eighth column $\left(E = \frac{1}{k}\sum_{1}^{k}(S_{real\_speed} - S_{estimated\_speed})^2\right)$.

Tab. 3: The results after 20 iterations.

Index	λ_1	λ_2	λ_3	λ_4	μ_1	μ_2	MSE
1	939.3539	434.0386	0.010616	0.002796	39.69101	12.90153	1.43543
2	939.3539	434.0386	0.010616	0.002796	39.69101	12.90153	1.43543
3	998.3147	240.8655	0.006058	5.00E-05	26.4032	8.702176	1.38273
4	998.3147	240.8655	0.006058	5.00E-05	26.4032	8.702176	1.38273
5	998.3147	240.8655	0.006058	5.00E-05	26.4032	8.702176	1.38273
6	1000	71.77744	0.001867	5.00E-05	6.31178	0.01	1.34914
7	1000	71.77744	0.001867	5.00E-05	6.31178	0.01	1.34914
8	1000	71.77744	0.001867	5.00E-05	6.31178	0.01	1.34914
9	1000	71.77744	0.001867	5.00E-05	6.31178	0.01	1.34914
10	1000	71.77744	0.001867	5.00E-05	6.31178	0.01	1.34914
11	1000	71.77744	0.001867	5.00E-05	6.31178	0.01	1.34914
12	1000	71.77744	0.001867	5.00E-05	6.31178	0.01	1.34914
13	1000	71.77744	0.001867	5.00E-05	6.31178	0.01	1.34914
14	1000	57.19251	0.00138	5.00E-05	0.01	0.01	1.33662
15	1000	57.19251	0.00138	5.00E-05	0.01	0.01	1.33662
16	1000	57.19251	0.00138	5.00E-05	0.01	0.01	1.33662
17	1000	57.19251	0.00138	5.00E-05	0.01	0.01	1.33662
18	1000	57.19251	0.00138	5.00E-05	0.01	0.01	1.33662
19	1000	53.48652	0.001293	5.00E-05	0.01	0.01	1.33568
20	1000	53.48652	0.001293	5.00E-05	0.01	0.01	1.33568

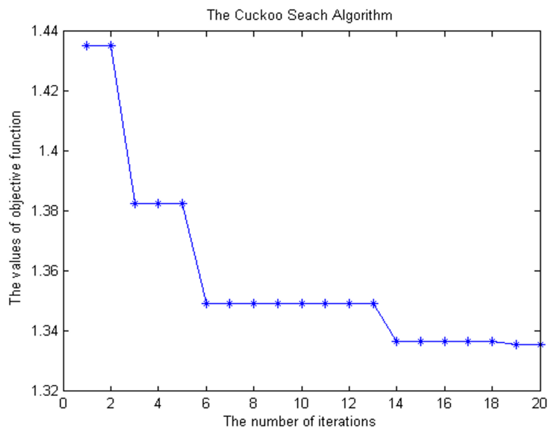

Fig. 7: The results of implementing the CSA algorithm after 20 iterations.

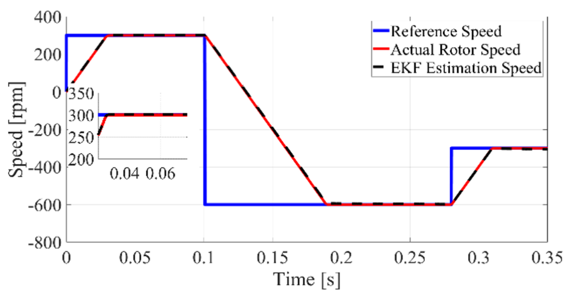

Fig. 8: The comparison of CSA-EKF estimation speed and actual rotor speed.

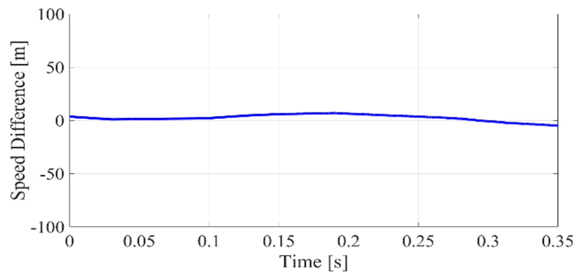

Fig. 9: The error between CSA-EKF estimation speed and actual rotor speed.

As the number of iterations increases, the parameters found will be better and the speed error will be smaller. In addition, Fig. 7 shows the results in an intuitively different form.

We take the parameters of the matrix Q (1000 53.48652 0.001293 5.00E-05) and R (0.01 0.01) that we found in the 20th run times and put them into the speed estimation model using the extended Kalman filter (EKF). After completing the simulation, the results of speed response and error are shown in Fig. 8 and Fig. 9.

With the parameters found by the CSA algorithm, the speed response is excellent, better than the trial and error solution, and the speed error is quite small. Using the CSA algorithm ensures the most optimal parameters and the smallest deviation. Tab. 4 compares the errors of the three methods mentioned above.

Tab. 4: The parameters of CSA algorithm.

The methods	MSE	The evaluated results
The random choice	2953.04194	Bad
The trial and error	55.75929	Good
The CSA-EKF	1.33568	The best

The data table above demonstrates that choosing the matrix Q, R at random provides a bad speed estimate, choosing the matrix Q, R by trial and error provides a pretty good speed estimate, but choosing Q, R with CSA algorithm, speed response estimation is the best.

4.3. The MRAS speed estimation model for the PMSM motor

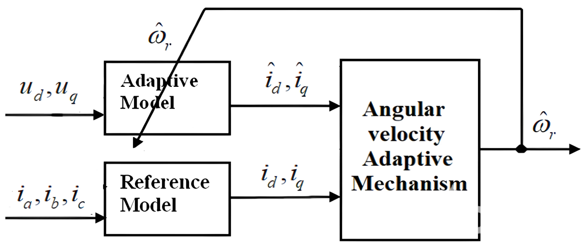

Fig. 10: The MRAS block diagram for the PMSM.

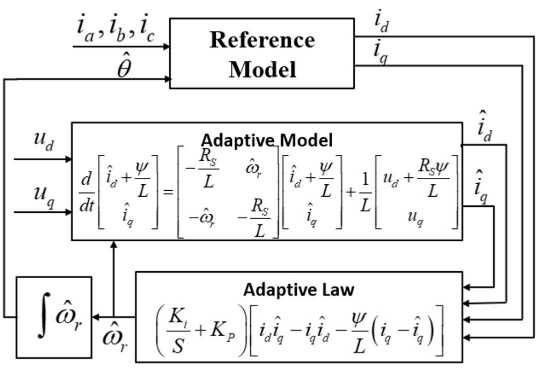

Fig. 11: The detailed MRAS model for the PMSM.

The MRAS model's characteristics [1–3] were outlined in the paper's introduction. Fig. 10 illustrates the block diagram of the MRAS model.

The equations and parameters of the MRAS model applied to the PMAS motor are detailed in Fig. 11.

From the equations in Fig. 11, we build the model in Matlab. The response of the speed estimation using MRAS under normal conditions is shown in Fig. 12.

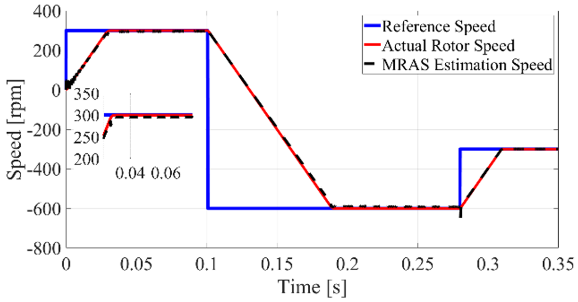

Fig. 12: The comparison of MRAS estimation speed and actual rotor speed of the PMSM.

The speed error of this MRAS model with the MSE standard is 4.92719, which is larger than the speed estimation model using the EKF model.

4.4. The speed estimated response using the MRAS and EKF models in case of impact noises

Process noise (w) is the noise generated from within the motor system, usually due to imperfect mathematical models of the system or due to difficult-to-predict physical factors. For example:

- Electromagnetic noise: Due to unstable rotor and stator magnetic flux.
- Load Torque Variation: Load changes unexpectedly while the motor is operating.
- Thermal Drift: Temperature affects the stator winding resistance.

Measurement noise (v) is the noise generated from measurements during data collection. For example:

- Sensor Noise: When measuring the rotor speed.
- Analog to Digital Converter: When converting current or voltage from analog to digital.
- Current Measurement Delay: Delay during current measurement.

In this section, we choose the change in stator resistance to represent process noise and white Gaussian noise (random number block on Matlab Simulink) to represent measurement noise in simulation.

1) The effect of white noise on the MRAS and EKF models

We apply Gaussian noise with a covariance value of 0.2 and a value of 1 to the currents id, iq of the speed estimation model using the MARS and EKF. The speed response obtained in the two models mentioned above is shown in Fig. 13 and Fig. 14.

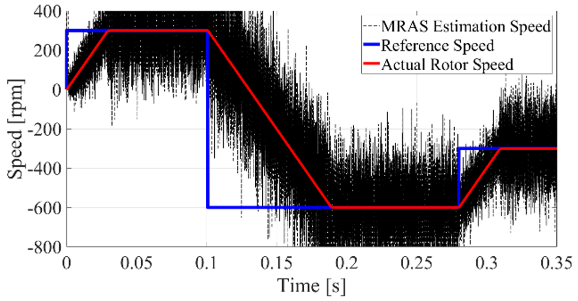

Fig. 13: The comparison of MRAS estimation speed and actual rotor speed with Gaussian noise.

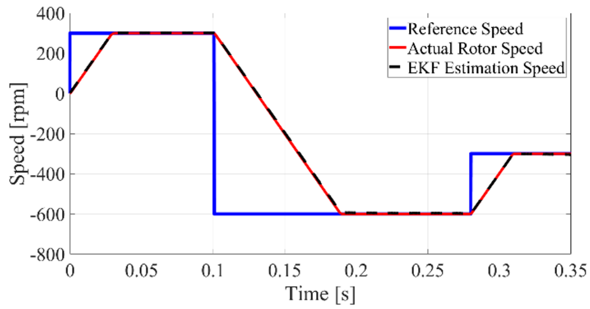

Fig. 14: The comparison of EKF estimation speed and actual rotor speed with Gaussian noise.

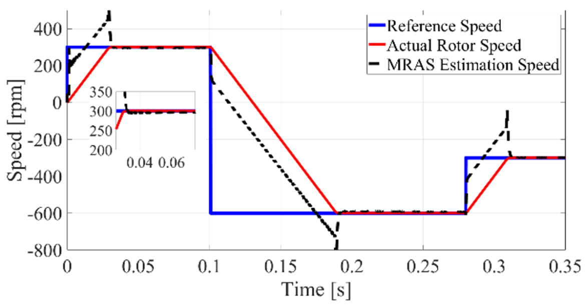

Fig. 15: The comparison of MRAS estimation speed and actual rotor speed with the stator resistance value increased by 200%.

The two responses shown in Fig. 13 and Fig. 14 illustrate that the MRAS model is significantly impacted by noise, resulting in a large speed estimation error of 1.7857e+03. In contrast, the EKF model is less affected by noise, leading to a smaller speed estimation error of 1.39663.

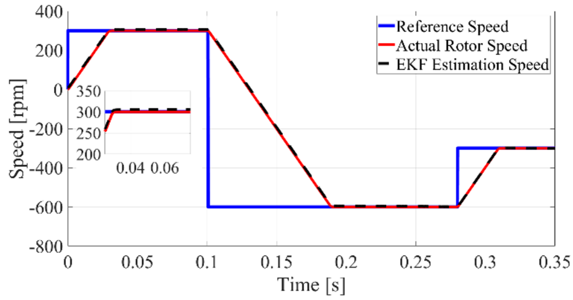

Fig. 16: The comparison of EKF estimation speed and actual rotor speed with the stator resistance value increased by 200%.

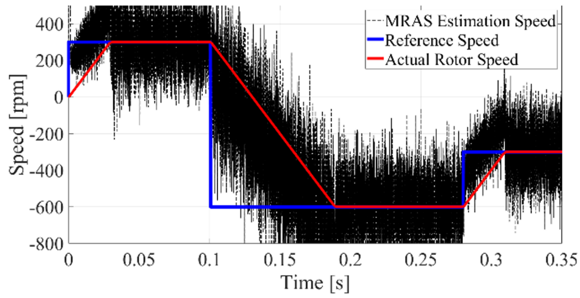

Fig. 17: The comparison of MRAS estimation speed and actual rotor speed with the stator resistance value increased by 200%. and white noise (its variance is 0.2).

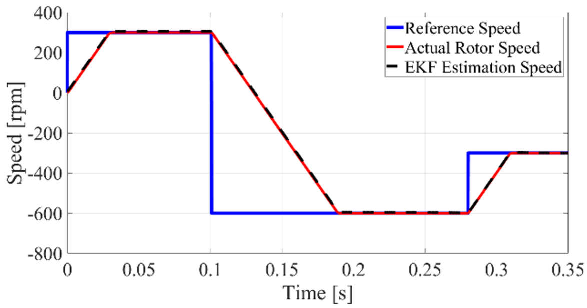

Fig. 18: The comparison of EKF estimation speed and actual rotor speed with the stator resistance value increased by 200% and white noise (its variance is 1.0).

2) The effect of changing stator resistance on the MRAS and EKF models

In this section, we investigate the system noise. For the testing, we select the resistance, changing the stator resistance from 0.05 Ω to 0.1 Ω, which represents a 200% increase. Figures 15 and 16 display the speed estimation responses for both the MRAS and EKF models.

From the above figures, the speed response of the MRAS model changes quite a lot (1.1738e+03). In contrast, the speed response of the EKF model changes

Tab. 5: The summary table of speed estimation error data of MRAS and EKF models:

Index	Rs	Variance for MRAS	Variance for Kalman	The MRAS model	The EKF model
1	Rs	0	0	4.92719	1.33568
2	Rs	0.2	1	1.7857e+03	1.39663
3	2Rs	0	0	1.1738e+03	2.25683
4	2Rs	0.2	1	3.1855e+03	2.40604

insignificantly (2.25683) when the stator resistance increases by 200%.

3) The effect of changing stator resistance and white noise on the MRAS and EKF models.

The speed response using the MRAS and EKF models in case of doubled stator resistance and white noise (variance of measurement noise is 0.2 for the MRAS model and 1.0 for the EKF model) is shown in Fig. 17 and 18.

When there are two types of noises: white noise and system noise, the speed response of the MRAS model (3.1855e+03) has a much larger error than the EKF model (2.40604).

From the above survey cases and the summary table, we can conclude that the EKF model, in addition to accurately estimating speed, also has better resistance to measurement noise and system noise than other estimation methods such as MRAS, etc.

5. Conclusion

This article presents how to estimate the speed of a PMSM motor controlled according to the field orientation (FOC) model using the EKF algorithm. Using the EKF filter to estimate speed has the advantage of being less dependent on motor parameters and more accurate than some other methods, such as MRAS, the sliding mode observer (SMO), however in this article, we emphasize determining the Q, R matrices in the EKF filter. The performance of the EKF filter depends heavily on the Q and R matrices. If the matrix is chosen randomly, the results are usually bad. If the matrix is selected using the trial and error method, the results achieved are relatively good, but it is time-consuming to choose and the results are not the most optimal value. Choosing the matrices Q and R using the CSA algorithm gives the best results. Furthermore, the EKF speed estimator demonstrates reduced sensitivity to measurement noise and system noise compared to other methods, such as MRAS. Simulation results on MATLAB Simulink provide data tables and graphs that prove this.

It can be seen that the suggested CSA-EKF model for the PMSM motor is less dependent on PMSM motor parameters than the MRAS models, but the CSA-EKF model is more complex than the above methods. The DSP processor (TMS320F2833x) is recommended when implementing the CSA-EKF algorithm for the PMSM motor. Today, this method can be easily implemented in industrial equipment due to the strong development of semiconductor technology.

Author Contributions

T. C. T. and P. B. created the model and designed and developed the method. Thinh built and wrote the program, collected data, and simulated results. T. C. T. and H. H. V. created and presented the published work, specifically writing the initial draft. All authors discussed the results and contributed to the final manuscript.

References

[1] WU, J., H. WEI, Y. ZHANG, H. WEI. Sensorless vector control of permanent magnet synchronous motor based on model reference adaptive system. *3rd IEEE International Conference on Computer and Communications (ICCC), Chengdu, China*. 2017, pp. 2879-2883. DOI: 10.1109/CompComm.2017.8323058.

[2] WEI, F., Y. WANG, Q. LIANG, Z. LI. Sensorless Control of Permanent Magnet Synchronous Motor Based on Improved Model Reference Adaptive System. *Chinese Automation Congress (CAC), Hangzhou, China*. 2019, pp. 2422-2426. DOI: 10.1109/CAC48633.2019.8997491.

[3] QUTUBUDDIN, M. D., N. YADAIAH. A new intelligent adaptive mechanism for sensorless control of permanent magnet synchronous motor drive. *Biologically Inspired Cognitive Architectures*. 2018, vol. 24, pp. 47-58. DOI: 10.1016/j.bica.2018.04.003.

[4] CHENXING, S., W. CHEN. Sensorless Vector Control of Three-Phase Permanent Magnet Syn-

chronous Motor Based on Model Reference Adaptive System. *IEEE 4th International Conference on Control Science and Systems Engineering (ICCSSE), Wuhan, China*. 2018, pp. 178-182. DOI: 10.1109/CCSSE.2018.8724849.

[5] WU, X., B. ZHANG. Sensorless Model Reference Adaptive Control of Permanent Magnet Synchronous Motor for Industrial Robots. *8th International Symposium on Next Generation Electronics (ISNE), Zhengzhou, China*. 2019, pp. 1-3. DOI: 10.1109/ISNE.2019.8896566.

[6] KAZRAJI, S. M., R. B. SOFLAYI, M. B. B. SHARIFIAN. Sliding-Mode Observer for Speed and Position Sensorless Control of Linear-PMSM. *Electrical, Control and Communication Engineering*. 2014, vol. 5, no. 1, pp. 20-26. DOI: 10.2478/ecce-2014-0003.

[7] YAO, G., L. XING, Y. HUANG. Sensorless Control Simulation of Permanent Magnet Synchronous Motor Based on Sliding Mode Observer. *IEEE 5th International Conference on Automation, Electronics and Electrical Engineering (AUTEEE), Shenyang, China*. 2022, pp. 688-693. DOI: 10.1109/AUTEEE56487.2022.9994354.

[8] CHEN, Y., T. FU, S. XING, R. TANG. Sensorless Control for Permanent Magnet Synchronous Motor Using Sliding Mode Observer. *6th World Congress on Intelligent Control and Automation, Dalian*. 2006, pp. 8079-8083. DOI: 10.1109/WCICA.2006.1713547.

[9] KOMMURI, S. K., et al. Higher-Order Sliding Mode Observer for Speed and Position Estimation in PMSM. *Mathematical Problems in Engineering*. 2014, vol. 2014, iss. 1. DOI: 10.1155/2014/589109.

[10] QIAN, Y., L. WEIGUO, L. GUANGZHAO. Backstepping Control of PMSM Based on RBF Neural Network. *International Conference on Electrical and Control Engineering, Wuhan, China*. 2010, pp. 5060-5064. DOI: 10.1109/iCECE.2010.1224.

[11] JIAO, L., et al. Research on PMSM Sensorless Control Based on Improved RBF Neural Network Algorithm. *37th Chinese Control Conference (CCC), Wuhan, China*. 2018, pp. 2933-2938. DOI: 10.23919/ChiCC.2018.8483974.

[12] LI, H., et al. Sensorless control of a PMSM based on an RBF neural network-optimized ADRC and SGHCKF-STF algorithm. *Measurement and Control*. 2023, vol. 57, iss. 3, pp. 266-279. DOI: 10.1177/00202940231195908.

[13] MERZOUG, M. S., H. BENALLA, H. NACERI. Speed Estimation Using Extended Filter Kalman for the Direct Torque Controlled Permanent Magnet Synchronous Motor (PMSM). *Second International Conference on Computer and Electrical Engineering, Dubai, United Arab Emirates*. 2009, pp. 122-127. DOI: 10.1109/ICCEE.2009.269.

[14] THINH, C. T., et al. Comparison of the speedy estimate methods of the induction motors. *TELKOMNIKA*. 2022, vol. 21, no. 1, pp. 223-234. DOI: 10.12928/TELKOMNIKA.v21i1.24089.

[15] TIAN, G., et al. Rotor Position Estimation of Sensorless PMSM Based on Extented Kalman Filter. *IEEE International Conference on Mechatronics, Robotics and Automation (ICMRA), Hefei, China*. 2018, pp. 12-16. DOI: 10.1109/ICMRA.2018.8490558.

[16] LI, H., Z. WANG. Sensorless Control for PMSM Drives Using the Cubature Kalman Filter based Speed and Flux Observer. *IEEE International Conference on Electrical Systems for Aircraft, Railway, Ship Propulsion and Road Vehicles & International Transportation Electrification Conference (ESARS-ITEC), Nottingham, UK*. 2018, pp. 1-6. DOI: 10.1109/ESARS-ITEC.2018.8607509.

[17] TONDPOOR, K., S. M. SAGHAIANNEZHAD, A. RASHIDI. Sensorless Control of PMSM Using Simplified Model Based on Extended Kalman Filter. *11th Power Electronics, Drive Systems, and Technologies Conference (PEDSTC), Tehran, Iran*. 2020, pp. 1-5. DOI: 10.1109/PEDSTC49159.2020.9088400.

[18] SHRIWASTAVA, R. G. Sensorless field-oriented control of PMSM drive system for automotive application. *International Journal of Electric and Hybrid Vehicles*. 2016, vol. 8, no. 3, pp. 213-224. DOI: 10.1504/IJEHV.2016.080015.

[19] THINH, C. T., et al. Parameters Estimation for Sensorless Control of Induction Motor Drive Using Modify GA and CSA Algorithm. *AETA 2018-Recent Advances in Electrical Engineering and Related Sciences: Theory and Application*. 2020, pp. 580-591. DOI: 10.1007/978-3-030-14907-9_57.

[20] IGLESIAS, A., et al. Cuckoo Search Algorithm with Lévy Flights for Global-Support Parametric Surface Approximation in Reverse Engineering. *Symmetry*. 2018, vol. 10, no. 3. DOI: 10.3390/sym10030058.

[21] LAAMARI, Y., K. CHAFAA, B. ATHAMENA. Particle swarm optimization of an extended Kalman filter for speed and rotor flux estimation of an induction motor drive. *Electrical engineering*. 2015, pp. 129-138. DOI: 10.1007/s00202-014-0322-1.